Comparing Internal Model Control and Sliding Mode Approaches for Vehicle Yaw Control

Massimo Canale, *Member, IEEE,* Lorenzo Fagiano, *Member, IEEE,* Antonella Ferrara, *Senior Member, IEEE,* and Claudio Vecchio,

***Abstract*—In this paper the problem of vehicle yaw control using a rear active differential is investigated. The proposed control structure employs a reference generator, designed to improve vehicle handling, a feedforward contribution which enhances the transient system response and a feedback controller. Due to system uncertainties and the wide range of operating situations, which are typical of the automotive context, a robust control technique is needed to guarantee system stability. Two different robust feedback controllers, based on Internal Model Control and Sliding Mode methodologies respectively, are designed and their performances are compared by means of extensive simulation tests, performed using a realistic 14 degrees of freedom model of the considered vehicle. The obtained results show the effectiveness of the proposed control structure with both feedback controllers and highlight their respective benefits and drawbacks. The presented comparative study is a first step to devise a new mixed control strategy able to exploit the benefits of both the considered techniques.**

***Index Terms*—Vehicle yaw control, Robust control, Internal Model Control, Sliding Mode control.**

I. Introduction

Vehicle yaw dynamics may show unexpected dangerous behaviour in presence of unusual external conditions and during emergency maneuvers, such as steering steps needed to avoid obstacles. Vehicle stability systems aim to ensure stability in such critical situations; moreover, in normal driving situations they can be used to improve the vehicle maneuverability. Different approaches to active chassis control have been proposed in the literature during recent years, see e.g. [1]-[8]. A common point to all solutions is the fact that the input variable may saturate due to actuator or tyre limits and this could deteriorate the control performances or cause vehicle instability. Moreover, the active control system has to guarantee safety (i.e. stability) performance robustly in presence of the uncertainties arising from the wide range of speed, load, etc., under which the vehicle operates. Robustness of active vehicle systems is a widely studied topic and interesting results have appeared (see e.g. [2] and [3]).

In this paper, the problem of yaw control is addressed considering a vehicle equipped with a Rear Active Differential (RAD) device. The proposed control structure employs a reference generator, designed to improve vehicle handling, a feedforward contribution and a feedback controller. The feedforward contribution is used to enhance system performances in the transient phase, while the feedback controller is designed in order to guarantee robust stability. In particular, the aim of this paper is to make a comparison between the results obtained with two different robust control techniques used to design the feedback controller, based on Internal Model Control (IMC) and Second Order Sliding Mode (SOSM) methodologies respectively. The choice of these two control methodologies is motivated by their robustness properties against the wide range of uncertainties which arise during vehicle operations. Internal Model Control techniques are well established control methodologies able to handle in an effective way both robustness (see [9]) and saturation (see e.g. [10]) issues. The enhanced Internal Model Control structure presented in [11], which guarantees robust stability as well as improved performances during saturation, will be employed. As for the sliding mode technique [12], its well-known robustness properties make this control methodology particularly suitable to deal with uncertain nonlinear time varying systems like the considered automotive system. Yet, conventional sliding mode control laws produce discontinuous control inputs [13] which can generate high frequency chattering, with the consequent excessive mechanical wear and passengers' discomfort, due to the propagation of vibrations throughout the different subsystems of the controlled vehicle. A possible counteraction to eliminate or, at least, reduce the vibrations induced by the controller consists in the approximation of the discontinuous control signals with continuous ones. However, this kind of solution makes the controlled system state evolve in a boundary layer of the ideal sliding subspace and all the appreciable features, which can induce the controller designer to rely on the sliding mode control methodology, are lost [13].

In order to circumvent the inconvenience of the vibrations induced by sliding mode controllers, a second order sliding mode control scheme [14], based on the so–called sub–optimal control algorithm [15], is designed. Second order sliding mode controllers generate continuous control actions, since the discontinuity is confined to the derivative of the control signal. Nevertheless, the generated sliding modes are ideal, in contrast to what happens for solutions which rely on continuous approximations of the discontinuous control laws. To compare and to show in a realistic way the effectiveness of the proposed control approaches, simulations will be performed using a detailed nonlinear 14 degrees of freedom vehicle model, which proved to give a good description of the

M. Canale and L. Fagiano are with Dipartimento di Automatica e Informatica, Politecnico di Torino, Corso Duca degli Abruzzi 24, 10129 Torino, Italy. E-mail addresses: massimo.canale@polito.it; lorenzo.fagiano@polito.it

A. Ferrara and C. Vecchio are with the Dipartimento di Informatica e Sistemistica, Università degli studi di Pavia, Via Ferrata 1, 27100 Pavia, Italy. E-mail addresses: antonella.ferrara@unipv.it; claudio.vecchio@unipv.it

vehicle dynamics as compared with real data.

II. Problem formulation and control requirements

The main aim of vehicle yaw control is to aid the driver to keep stability in critical maneuvers and in presence of unusual external conditions. In such a contribution, in order to introduce the control requirements, some basic concepts of lateral vehicle dynamics are now recalled. Vehicle inputs are the steering angle $\delta(t)$, commanded by the driver, and external forces and moments applied to the vehicle centre of gravity. The most significant variables describing the behaviour of the vehicle are its speed $v(t)$, lateral acceleration $a_y(t)$, yaw rate $\dot{\psi}(t)$ and side slip angle $\beta(t)$. As a first approximation, considering car and suspension system as a rigid body moving at constant speed v, the following relationship links $a_y(t)$ to $\dot{\psi}(t)$ and $\dot{\beta}(t)$:

$$a_y(t) = v(\dot{\psi}(t) + \dot{\beta}(t)) \tag{1}$$

In steady state motion (i.e. $\dot{\beta}(t) = 0$), lateral acceleration is proportional to yaw rate through the vehicle speed. In this situation, let us consider the uncontrolled car behaviour: for each constant speed value, by means of standard steering pad maneuvers it is possible to obtain the steady state lateral acceleration corresponding to different values of the steering angle. These values can be graphically represented on the *steering diagram* (see Fig. 1, dotted line) where the steering angle $\delta(t)$ is reported with respect to the lateral acceleration. Such curves are mostly influenced by road friction and depend on the tyre lateral force-slip characteristics. At low acceleration the shape of the steering diagram is linear and its slope is a measure of the readiness of the car: the lower this value, the higher the lateral acceleration reached by the vehicle with the same steering angle, the better the maneuverability and handling quality perceived by the driver (see e.g. [16]). At high acceleration the behaviour becomes nonlinear showing a saturation value, that is the highest lateral acceleration the vehicle can reach. The intervention of an active differential device can be considered as a yaw moment $M_z(t)$ acting on the car centre of gravity: such a moment is able to vary, under the same steering conditions, the behaviour of a_y, modifying the steering diagram according to some desired requirements. Thus, a target steering diagram (as shown in Fig. 1, solid line) can be introduced to take into account the performance improvements to be obtained by the control system. In particular, in this work such reference curves are chosen in order to decrease the steering diagram slope in the linear tract (which is related to the vehicle understeer gradient, see [17]), thus improving the vehicle maneuverability, and to increase the maximum lateral acceleration that can be reached. More details about the generation of such target steering diagrams are reported in Section IV-A and in amore extended form in [8]. Then, reference yaw rate values can be derived from the target steering diagrams, using equation (1) with $\dot{\beta} = 0$.

Therefore, the choice of yaw rate as the controlled variable is justified, also considering its reliability, since the measure

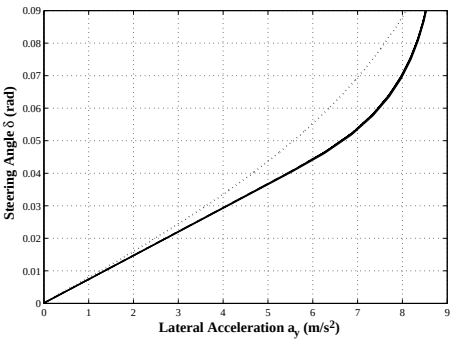

Fig. 1. Uncontrolled vehicle (dotted), and target (solid) steering diagrams. Vehicle speed: 100 km/h

of yaw rate is less noisy than lateral acceleration and it is not subject to disturbances due to e.g. lateral road inclination. A reference generator will provide the values for $\dot{\psi}$ needed to achieve the desired performances by means of a suitably designed feedback control law.

As for the generation of the required yaw moment $M_z(t)$, in this paper a full Rear Active Differential (RAD) is used (see [8], [18] and [19] for details). The main advantage of this system is the capability of generating yaw moments of every value within the actuation system saturation limits, regardless of the input driving torque value and the speed values of the rear wheels. The considered device has a yaw moment saturation value of ± 2500 Nm, due to the physical limits of its electro-hydraulic system.

In addition to the objective of improving the steady–state vehicle maneuverability, the dynamic vehicle behaviour needs to satisfy good damping and readiness properties, which can be taken into account by a proper design of the feedback controller and the use of a feedforward action based on the driver input (i.e. δ) to increase system readiness. Needless to say that at least safety (i.e. stability) requirements have to be guaranteed in presence of the uncertainty arising from the wide range of the vehicle operating conditions of speed, load, tyre, friction, etc. This can be achieved using a controller whose design procedure takes into account the effects of model uncertainty. In particular, in this paper a SOSM controller and the enhanced IMC scheme introduced in [11] and proposed in [8] for vehicle stability control will be employed and their performances will be compared. Both these controllers are able to handle robust stability as well as saturation issues, as it will be described in Sections IV-B and IV-C.

III. Model description

In both the considered control techniques, the controller design will be worked out on the basis of a single track vehicle model (see Fig. 2). The model dynamic equations are the following (see e.g. [17]):

$$\begin{aligned} mv(t)\dot{\beta}(t) + mv(t)\dot{\psi}(t) &= F_{yf,p}(t) + F_{yr,p}(t) \\ J_z\ddot{\psi}(t) &= aF_{yf,p}(t) - bF_{yr,p}(t) + M_z(t) \end{aligned} \tag{2}$$

where m is the vehicle mass, J_z is the moment of inertia around the vertical axis, l is the wheel base, a and b are the distances between the centre of gravity and the front and

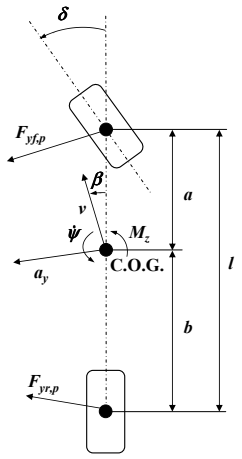

Fig. 2. Single track schematic.

rear axles respectively. $F_{yf,p}$ and $F_{yr,p}$ are the front and rear tyre lateral forces. In order to take into account the dynamic generation mechanism of tyre forces, the following first–order equations are also added:

$$\begin{aligned} F_{yf,p}(t) + l_f/v\dot{F}_{yf,p}(t) &= -c_f(\beta(t) + a\dot{\psi}(t)/v(t) - \delta(t)) \\ F_{yr,p}(t) + l_r/v\dot{F}_{yr,p}(t) &= -c_r(\beta(t) - b\dot{\psi}(t)/v(t)) \end{aligned} \tag{3}$$

where l_f and l_r are the front and rear tyre relaxation lengths and c_f and c_r are the front and rear tyre cornering stiffnesses. As already pointed out, the real vehicle behaviour is influenced by several different factors that introduce model uncertainty. Therefore, in order to perform a robust design, uncertainty intervals are considered for tyre parameters (0% to -20% front, 0% to +20% rear tyre cornering stiffness and $\pm$ 10% tyre relaxation lengths variations with respect to their nominal values), vehicle speed ($\pm$ 30% of the nominal value) and vehicle mass (0% to +25% of the nominal value with consequent geometrical and inertial parameters changes). Suitable descriptions of system dynamics and related uncertainty will be introduced in Sections IV-B and IV-C, according to the considered control design technique.

IV. Control design

The proposed control structure is depicted in Fig. 3. In such

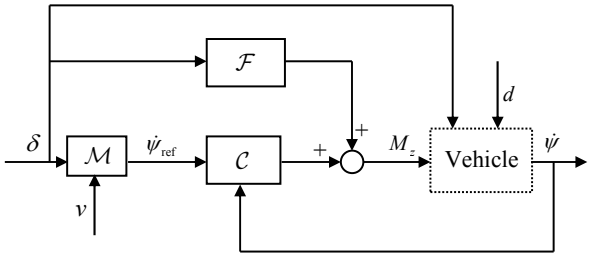

Fig. 3. Considered control structure.

a structure, the desired yaw rate behaviour is imposed by the yaw rate reference signal $\dot{\psi}_{\text{ref}}(t)$ which is generated by a static map $\mathcal{M}$ using the values of $\delta(t)$ and $v(t)$. The feedback controller $\mathcal{C}$ computes the yaw moment contribution needed to follow the required yaw rate performances described by $\dot{\psi}_{\text{ref}}(t)$. The external input $d(t)$ accounts for disturbances like lateral wind forces, different road conditions etc.. Controller $\mathcal{C}$ is designed according to either IMC or SOSM methodologies. To compare the two approaches, the same reference map $\mathcal{M}$ is employed with both controllers. Moreover, to improve the yaw rate dynamic properties exploiting the knowledge of the driver input, a feedforward contribution $\mathcal{F}$ from $\delta(t)$ has been added too. Note that, due to the different interaction of the feedforward controller with the considered IMC and SOSM feedback control laws, two different filters $\mathcal{F}$ are designed, in order to obtain the best performances in each case.

A. Reference generator

The reference yaw rate value is generated using a nonlinear static map $\dot{\psi}_{\text{ref}} = \mathcal{M}(\delta, v)$ which uses as inputs the steering angle $\delta(t)$ and the vehicle speed $v(t)$. In order to compute the map values, a single track nonlinear steady state vehicle model is considered (see [8]). The model equations are the following:

$$\begin{aligned} m\,a_y = m\,v\,\dot{\psi} &= F_{yf,p}(\alpha_f) + F_{yr,p}(\alpha_r) \\ aF_{yf,p}(\alpha_f) - bF_{yr,p}(\alpha_r) + M_z &= 0 \end{aligned} \tag{4}$$

where the front and rear tyre lateral forces $F_{yf,p}$ and $F_{yr,p}$ are computed considering the nonlinear tyre slip-lateral force relationship introduced in [20]:

$$\begin{aligned} F_{yf,p}(\alpha_f) = D_f(C_f \arctan(B_f(\alpha_f) - E_f(B_f(\alpha_f) \\ - \arctan(B_f(\alpha_f))))) \\ F_{yr,p}(\alpha_r) = D_r(C_r \arctan(B_r(\alpha_r) - E_r(B_r(\alpha_r) \\ - \arctan(B_r(\alpha_r))))) \end{aligned} \tag{5}$$

where α_f, α_r are the front and rear tyre sideslip angles respectively, which can be approximated as:

$$\begin{aligned} \alpha_f &= \beta + a\dot{\psi}/v - \delta \\ \alpha_r &= \beta - b\dot{\psi}/v \end{aligned}$$

Coefficients B_f, C_f, D_f, E_f, B_r, C_r, D_r, E_r can be identified, for a given uncontrolled vehicle, using the experimental data collected during standard handling maneuvers: the values employed in this work are reported in Section V. For each constant speed value v, the reference map $\mathcal{M}(\delta, v)$ is derived with a two–step procedure. At first, equations (4) are numerically solved to obtain the uncontrolled vehicle steering diagram, i.e. the value of $a_y = \dot{\psi}\,v$ as function of the steering angle δ, with $M_z = 0$. Note that, since the tyre equations $F_{yf,p}(\cdot)$, $F_{yr,p}(\cdot)$ are not invertible in general (see e.g. [21]), two solutions of equations (4) can be found, given the same value of δ. However, only one of such solutions corresponds to a stable equilibrium point and it is therefore selected by the numerical procedure. In the second step, the reference steering diagram is chosen according to some criteria, like improvement of the maneuverability with respect to the uncontrolled vehicle, as already pointed out in Section II (see [8] for more details). Note that in steady state conditions equation $a_y = v\,\dot{\psi}$ holds, thus a reference value of a_y, given by the reference steering diagram, directly corresponds to a value of $\dot{\psi}_{\text{ref}}$. Indeed, equations (4) are also employed to verify that the chosen

reference steering diagram corresponds to feasible vehicle motion conditions, according to the actuator and tyre limits. A reference steering diagram is designed for each value of v, so a map of values of $\dot{\psi}_{\text{ref}}$ is computed.

B. IMC controller design

The design of the feedback controller in the case of Internal Model Control approach relies on H_∞ methodologies, to guarantee robust stability in presence of model uncertainty. In order to exploit this design technique, a linear model and an unstructured description of the related uncertainty in the frequency domain are needed. By applying the Laplace transform and straightforward manipulations to the vehicle model equations (2)–(3), the following transfer functions are obtained:

$$\dot{\psi}(s) = G_\delta(s)\delta(s) + G_M(s)M_z(s) \tag{6}$$

As the control input is the yaw moment M_z and the controlled output is the yaw rate $\dot{\psi}$, transfer function $G_M(s)$ is used in the IMC feedback controller design. In this framework, the considered model uncertainty is described by means of an additive linear model set of the form (see e.g. [22], [23]):

$$\mathcal{G}_M(G_M, \Gamma(\omega)) = \{G_M(s) + \Delta(s) : |\Delta(j\omega)| \leq \Gamma(\omega)\} \tag{7}$$

where $\Delta(s)$ is the considered model uncertainty, whose magnitude is bounded by function $\Gamma(\omega)$. In order to derive such model set, simulation data have been used. Such data have been generated using an accurate 14 degrees of freedom nonlinear model and considering the effects of the parameter uncertainty introduced in Section III. The model set obtained for the considered vehicle is reported in Fig. 7 of Section V. IMC techniques (see [9]) based on H_∞ optimization are able to satisfy robust stability requirements in presence of input saturation (see e.g. [11]). A generic IMC structure is reported in Fig. 4. However, as discussed in [10], IMC control may

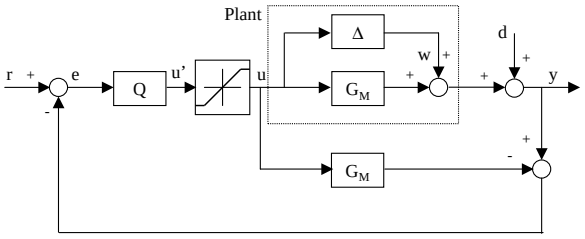

Fig. 4. IMC scheme with model uncertainty and saturating input.

deteriorate the system performances when saturation is active, even in absence of model uncertainty. In order to improve the performances under saturation, an enhanced robust IMC structure based on the anti-windup solutions presented in [10] has been proposed in [11]. The control scheme considered in [11] gives rise to a nonlinear controller $\mathcal{Q}$, which replaces the linear controller $Q(s)$ in Fig. 4, made up by the cascade connection of a linear filter $Q_1(s)$ and a non linear loop $\mathcal{Q}_2$ as shown in Fig. 5. The design procedure can be summarized in the following steps:

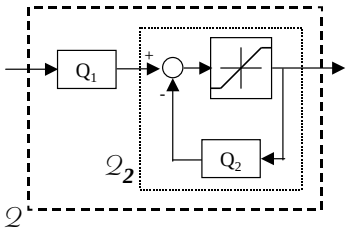

Fig. 5. Nonlinear IMC enhanced controller.

1) A preliminary robust IMC controller $Q(s)$ is computed solving the following H_∞ optimization problem:
$$\begin{aligned} &Q(s) = \arg\min \left\| W_S^{-1}(s)\left(1 - G_M(s)\,Q(s)\right)\right\|_\infty \\ &\text{s.t.} \left\| Q(s)\,\bar{\Gamma}(s)\right\|_\infty < 1 \end{aligned} \tag{8}$$
where $\bar{\Gamma}(s)$ is suitable rational function with real coefficients, stable, whose magnitude strictly overbounds the frequency course $\Gamma(\omega)$ and $W_S(s)$ is a weighting function introduced to take into account a desired specification on the sensitivity function $(1 - G_M(s)Q(s))$
2) Using controller $Q(s)$ computed in the previous step, a controller $Q_2(s)$, via the design of a preliminary filter $\bar{Q}_1(s)$, is obtained according to the criteria introduced in [10]. It has to be noted that $Q_2(s)$ must ensure the stability of the non linear loop $\mathcal{Q}_2$ (see Fig. 5). To this end, an upper bound $\gamma_{\mathcal{Q}_2}$ on the H_∞ norm of $\mathcal{Q}_2$ has to be computed (see [11] for details). If $\gamma_{\mathcal{Q}_2}$ is finite then the stability of $\mathcal{Q}_2$ is guaranteed. In case that the stability of $\mathcal{Q}_2$ is not assured then a new IMC controller design has to be performed starting from point 1).
3) Then, the linear controller $Q_1(s)$ can be designed by means of the following H_∞ optimization problem:
$$\begin{aligned} &Q_1(s) = \arg\min \left\| W_S^{-1}(s)\left(1 - G_M(s)\tfrac{Q_1(s)}{1+Q_2(s)}\right)\right\|_\infty \\ &\text{s.t.} \|Q_1(s)\bar{\Gamma}(s)\,\gamma_{\mathcal{Q}_2}\|_\infty < 1 \end{aligned} \tag{9}$$

As already pointed out, in order to improve the yaw rate transient response a further control input is added. Such control action is generated by a feedforward controller driven by the steering angle $\delta(t)$. The feedforward controller is computed by means of a linear filter $F^{\text{IMC}}(s)$, designed to match the open loop yaw rate behaviour, given by (6), with the one described by an objective transfer function $T_\delta^{\text{des,IMC}}(s)$:

$$\dot{\psi}(s) = T_\delta^{\text{des,IMC}}(s)\delta(s) \tag{10}$$

In this way, considering relation (6), where $M_z(s)$ is computed as $M_z(s) = F^{\text{IMC}}(s)\delta(s)$ and $\dot{\psi}(s)$ is given by (10), the feedforward filter $F^{\text{IMC}}(s)$ is derived as:

$$F^{\text{IMC}}(s) = \frac{T_\delta^{\text{des,IMC}}(s) - G_\delta(s)}{G_M(s)} \tag{11}$$

Transfer function $T_\delta^{\text{des,IMC}}(s)$ is chosen according to the desired open loop system response. Note that $T_\delta^{\text{des,IMC}}(s)$ must be such that the filter $F^{\text{IMC}}(s)$ is a proper transfer function. Moreover, as the feedforward controller aims to enhance the transient response only, its contribution should be deactivated

in steady state conditions. This is achieved when the dc-gains of $T_\delta^{\text{des,IMC}}(s)$ and $G_\delta(s)$ are the same. The proposed procedure for feedforward design does not take explicitly into account the presence of the feedback controller. Therefore, the weighting function $W_S(s)$ in (8)–(9), employed in the IMC design, and $T_\delta^{\text{des,IMC}}(s)$ in (11), used for the feedforward design, are adjusted using simulation/experiments, in order to obtain the best overall performance.

Note that if the feedforward action had been implemented as shown in Fig. 3, the improvements introduced during saturation by the structure of Fig. 5 would influence only the feedback control contribution. This may cause a slight degradation on the control performance. In order to avoid such a degradation, in the case of IMC controller the feedforward contribution is injected at the reference level, obtaining the control scheme reported in Fig. 6. In such a structure, the

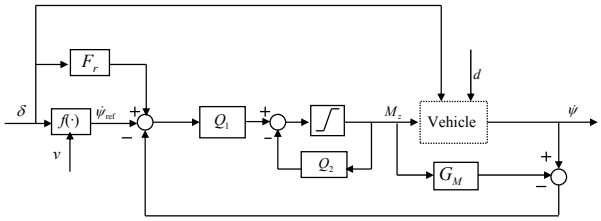

Fig. 6. The proposed control scheme for IMC control system.

feedforward action is realized by the linear filter $F_r(s)$, whose expression can be computed by straightforward manipulations as:

$$F_r(s) = \left(\frac{1 + Q_2(s)}{Q_1(s)} - G_M(s) \right) F^{\text{IMC}}(s) \tag{12}$$

C. SOSM controller design

A Second Order Sliding Mode (SOSM) is a movement of a dynamic system confined to a particular subspace, named sliding manifold, which can be mathematically described in Filippovs' sense [24]. The SOSM is determined by

$$S(x) = \dot{S}(x) = 0 \tag{13}$$

where $S(x)$, the so–called sliding variable, is a smooth function of the state x of the considered dynamical system, and $S(x) = 0$ identifies the sliding manifold. SOSM control generalizes the basic sliding mode control idea, acting on the second order time derivative of the system deviation from the sliding manifold, instead that on the first deviation derivative, as it happens in first order sliding mode control design [13]. The main advantage of SOSM control [14], with respect to the first order case, is that it generates a continuous control action, while keeping the same robustness with respect to matched uncertainties.

The chosen sliding variable is the error between the actual yaw rate and the reference yaw rate, i.e.,

$$S(t) = \dot\psi(t) - \dot\psi_{\text{ref}}(t) \tag{14}$$

since the control objective is to make this error vanish in finite time. The first and second time derivative of the sliding variable are, respectively

$$\begin{cases} \dot S(t) &= (aF_{yf,p}(t) - bF_{yr,p}(t) + M_z(t))/J_z - \ddot\psi_{\text{ref}}(t) \\ \ddot S(t) &= (a\dot F_{yf,p}(t) - b\dot F_{yr,p}(t) + \dot M_z(t))/J_z - \dddot\psi_{\text{ref}}(t) \end{cases} \tag{15}$$

Introducing the auxiliary variables $y_1(t) = S(t)$ and $y_2(t) = \dot S(t)$, system (15) can be rewritten as

$$\begin{cases} \dot y_1(t) &= y_2(t) \\ \dot y_2(t) &= \lambda(t) + \tau(t) \end{cases} \tag{16}$$

where $\tau(t) = \dot M_z(t)/J_z$ is the auxiliary control and $\lambda(t) = (a\dot F_{yf,p}(t) - b\dot F_{yr,p}(t))/J_z - \dddot\psi_{\text{ref}}(t)$. On the basis of physical considerations, the quantity $\lambda(t)$ is bounded. Moreover, to apply the SOSM algorithm it is not necessary that a precise evaluation of $\lambda(t)$ (which can be not easy to compute) is available. In the sequel, it will be only assumed that a suitable bound of $\lambda(t)$ is known, i.e.:

$$|\lambda(t)| \le \Lambda \tag{17}$$

A conservative estimation for Λ can be determined on the basis of (2)–(3) and of the uncertainty intervals considered for the vehicle and tyre parameters (see Section III). According to the SOSM sub–optimal control algorithm [15], the auxiliary control variable τ is defined as

$$\tau(t) = \dot M_z(t)/J_z = -K_{SL}\ sign(S(t) - \frac{1}{2}S_M(t)) \tag{18}$$

where $S_M(t)$ is a piece–wise constant function representing the value of the last singular point of $S(t)$ (i.e. its most recent value $S(t_{Mi})$ such that $\dot S(t_{Mi}) = 0$) and K_{SL} is a design parameter. To ensure robust stability, K_{SL} must satisfy

$$K_{SL} > 2\Lambda \tag{19}$$

The control law (18) is a sub–optimal second order sliding mode control law. So, by following a theoretical development as that provided in [15] for the general case, it can be proved that the trajectories on the y_1Oy_2 plane are confined within limit parabolic arcs including the origin. The absolute values of the coordinates of the trajectory intersections with the y_1, and y_2 axis decrease in time. As shown in [15], under condition (19) the following relationships hold

$$|y_1(t)| \le |S_M(t)| \qquad |y_2(t)| \le \sqrt{|S_M(t)|}$$

and the convergence of $S_M(t)$ to zero takes place in finite time [15]. As a consequence, also $y_1(t)$ and $y_2(t)$ tend to zero in finite time since they are both bounded by $\max(|S_M(t)|, \sqrt{|S_M(t)|})$.

As regards the feedforward contribution, such action is computed as:

$$F^{\text{SL}}(s) = \frac{T_\delta^{\text{des,SL}}(s) - G_\delta(s)}{G_M(s)} \tag{20}$$

In a way similar to the case of IMC, transfer function $T_\delta^{\text{des,SL}}(s)$ is a design parameter describing the desired open loop system behaviour, chosen such that transfer function $F^{\text{SL}}(s)$ is proper. Moreover, the dc-gains of $T_\delta^{\text{des,SL}}(s)$ and $G_\delta(s)$ have to be the same, in order to deactivate the feedforward contribution in steady state conditions. Equation (20) is obtained like equation (11) and it does not take explicitly

into account the presence of the sliding mode controller: thus, the SOSM design parameter K_{SL} (18) and function $T_\delta^{\text{des,SL}}(s)$ (11) are tuned using simulation/experiments, in order to obtain the best overall performance. Filter $F^{\text{SL}}(s)$ is implemented as shown in Fig. 3.

In order to take into account the saturation of the control input, in accordance to [25], the actual control law $M_z(t)$ is given by

$$\dot{M}_z(t) = \begin{cases} -M_z(t) & \text{if } |M_z(t)| \geq M_{z,\text{sat}} \\ J_z \tau(t) & \text{otherwise} \end{cases} \quad (21)$$

where $\tau(t)$ is given by (18) and $M_{z,\text{sat}}$ is the saturation value of the RAD, i.e., 2500 Nm.

V. Simulation results

The IMC control design has been performed using transfer functions $G_\delta(s)$ and $G_M(s)$ defined in (6) computed at a nominal speed $v = 100\,\text{km/h} = 27.77\,\text{m/s}$ and with the following values of the other involved parameters:

$m = 1715\,\text{kg}$ $J_z = 2700\,\text{kgm}^2$ $a = 1.07\,\text{m}$ $b = 1.47\,\text{m}$ $l_f = 1\,\text{m}$ $l_r = 1\,\text{m}$ $c_f = 95117\,\text{Nm/rad}$ $c_r = 97556\,\text{Nm/rad}$

The tyre slip–force characteristics (5) have been computed with the following parameters:

$B_f = 7.8$, $C_f = 1.3$, $D_f = 8824.5$, $E_f = -0.29$

$B_r = 13.0$, $C_r = 1.3$, $D_r = 6725.1$, $E_r = -0.16$

The computed model set (7) is shown in Fig. 7, where the nominal transfer function magnitude behaviour is reported and compared with the obtained uncertainty bounds. The following

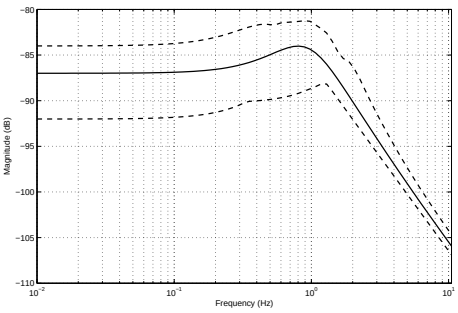

Fig. 7. Model set $\mathcal{G}_M$: Nominal transfer function G_M (solid) and upper and lower uncertainty bounds (dashed).

weighting function $W_S(s)$ has been used in the optimization problem (8):

$$W_S(s) = \frac{s}{s+20} \quad (22)$$

Finally, in the feedforward design, the transfer function $T_\delta^{\text{des,IMC}}(s)$ has been chosen as:

$$T_\delta^{\text{des,IMC}}(s) = \frac{5.67}{1+\frac{s}{6}}$$

Transfer function $Q_2(s)$, employed in the anti-windup structure of the IMC controller, is the following:

$$Q_2(s) = \frac{72\,(s+39.13)\,(s+1.126)\,(s^2+21.85\,s+157)}{(s+54)(s^2+47.16\,s+562.3)(s^2+8.392\,s+61.89)}$$

Note that $Q_2(s)$ has to be strictly proper due to implementation issues.

As regards the Sliding Mode controller design, the value of the gain K_{SL} in (18) has been chosen as:

$$K_{\text{SL}} = 5000$$

while the employed objective function $T_\delta^{\text{des,SL}}(s)$ is:

$$T_\delta^{\text{des,SL}}(s) = \frac{5.67}{1+\frac{s}{10}}$$

Functions $W_S(s)$, $T_\delta^{\text{des,IMC}}(s)$, K_{SL} and $T_\delta^{\text{des,SL}}(s)$ have been chosen through simulations, to obtain the best performance for each control strategy.

In order to show in a realistic way the performance obtained by the proposed yaw control approaches, simulations have been performed using a detailed nonlinear 14 degrees of freedom Simulink model. The model degrees of freedom correspond to the standard three chassis translations and yaw, pitch and roll angles, the four wheel angular speeds and the four wheel vertical movements with respect to the chassis. Nonlinear characteristics, obtained on the basis of measurements on the real vehicle, have been employed to model the tyre, steer and suspension behaviour. In the following tests, either the nominal vehicle configuration or a vehicle with increased mass (up to +300 kg, with consequent inertial and geometrical parameter variations) have been considered.

A. Constant speed steering pad

The aim of this maneuver is to evaluate the steady–state vehicle performance: the steering angle is slowly increased (i.e. $1^\circ/\text{s}$ handwheel velocity), while the vehicle is moving at constant speed, until the vehicle lateral acceleration limit (about 8.6 m/s^2) is reached and the vehicle becomes unstable or the constant speed value cannot be kept. The results of this test, performed at 90 km/h with an increased mass (+300 kg) vehicle, are shown in Fig. 8, in terms of relative tracking error $(\dot{\psi}_{\text{ref}} - \dot{\psi})/\dot{\psi}_{\text{ref}}$: it can be noted that a smooth behavior is obtained for the IMC control, while a chattering phenomenon occurs in the case of sliding mode controller. The chattering effect is due to the fact that the presence of the RAD actuator increases the relative degree of the system. As a consequence, the transient process converge to a periodic motion in a small vicinity of the sliding surface [26]. Such a course is typical for Sliding Mode control and it represents a drawback of this control strategy. However, in the considered case the oscillations are too small ($\pm$ 0.04 %) to be perceived by the driver. A possible way to reduce chattering is the use of lower values of the gain K_{SL} in the computation of the auxiliary control (18): however, the lower K_{SL} the worse the performance and robustness properties of the SOSM controller [15]. Thus, a compromise has to be chosen in SOSM controller, between limited chattering and good performances. The results of a more complete analysis of the tracking performances obtained with the considered control strategies, for the steering pad maneuver, are reported in Tables I–II, in terms of maximum error E_{max} and root mean square error E_{rms}:

$$E_{\text{max}} = \max_{t \in [t_0, t_{\text{end}}]} |\dot{\psi}_{\text{ref}}(t) - \dot{\psi}(t)| \quad (23)$$

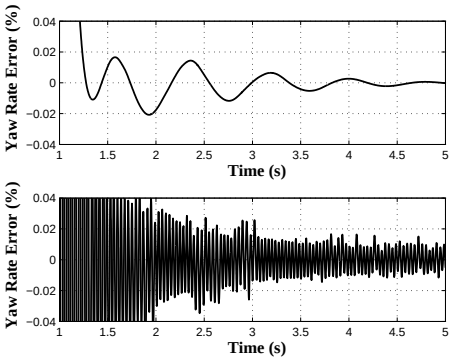

Fig. 8. Steering pad test at 90 km/h. Relative tracking error behavior during the initial part of the test for the IMC (upper) and Sliding Mode (lower) control systems with increased mass (+300 kg) vehicle.

TABLE I
MAXIMUM REFERENCE TRACKING ERRORS: STEERING PAD MANEUVER AT 100 KM/H

$E_{\max}$	+300 kg	+200 kg	+100 kg	Nominal
IMC	$1.6 \cdot 10^{-4}$	$1.6 \cdot 10^{-4}$	$1.5 \cdot 10^{-4}$	$1.4 \cdot 10^{-4}$
SOSM	$6.0 \cdot 10^{-4}$	$6.6 \cdot 10^{-4}$	$6.8 \cdot 10^{-4}$	$2.3 \cdot 10^{-4}$

$$E_{\text{rms}} = \sqrt{\frac{1}{t_{\text{end}} - t_0} \int_{t_0}^{t_{\text{end}}} (\dot{\psi}_{\text{ref}}(t) - \dot{\psi}(t))^2 dt}$$

where t_0 and t_{end} are the starting and final test time instants respectively. It can be noted that both controllers are able to achieve good tracking performance, with very low values of E_{rms} and $E_{\max}$. The best results are obtained with the IMC controller, which appears to be more suited for the considered steady–state maneuver. Similar results have been obtained for different speed values.

B. Steer reversal test

This test aims to evaluate the controlled car transient response performances: in Fig. 9 the employed steering angle behaviour is showed, corresponding to a maximum handwheel angle of 50°, with a handwheel speed of 400°/s. The maneuver has been performed at 100 km/h. The obtained yaw rate course shows that the controlled vehicle dynamic response in nominal conditions is well damped with both the Sliding Mode and the IMC controllers. The course of yaw moment M_z is reported in Fig. 11: again it can be noted that chattering of the control variable occurs with the Sliding Mode controller, while a smooth behaviour is obtained with the IMC controller. On the other hand, the control input issued by the IMC controller saturates in all the transients during the test, while the Sliding Mode controller is less aggressive. Both control systems are

TABLE II
RMS REFERENCE TRACKING ERRORS: STEERING PAD MANEUVER AT 100 KM/H

E_{rms}	+300 kg	+200 kg	+100 kg	Nominal
IMC	$6.0 \cdot 10^{-10}$	$6.6 \cdot 10^{-10}$	$8.6 \cdot 10^{-10}$	$1.2 \cdot 10^{-9}$
SOSM	$4.0 \cdot 10^{-8}$	$4.2 \cdot 10^{-8}$	$4.9 \cdot 10^{-8}$	$2.8 \cdot 10^{-7}$

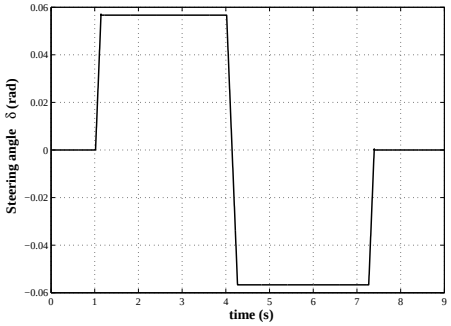

Fig. 9. Steering angle reversal test input corresponding to 50° handwheel angle

able to handle saturation effectively, without worsening of the performance. Table III shows the tracking performance

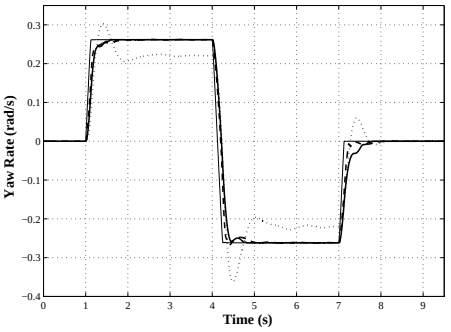

Fig. 10. 50° steer reversal test at 100 km/h, nominal conditions. Comparison between the reference yaw rate course (thin solid line) and the ones obtained with the uncontrolled (dotted) vehicle and the Sliding Mode (solid) and IMC (dashed) controlled vehicles.

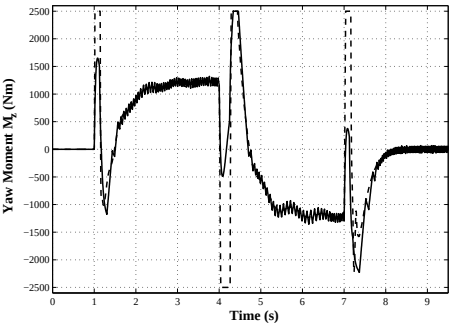

Fig. 11. 50° steer reversal test at 100 km/h, nominal conditions. Comparison between the yaw moment courses obtained with the Sliding Mode (solid) and IMC (dashed) controllers.

obtained in the 50° steer reversal maneuver with varying mass values, with consequent changes of the other inertial and geometrical parameters, in terms of root mean square error E_{rms} (23). Both controllers achieve low values of E_{rms} also with increased mass, showing good robustness properties. In this case, the difference between IMC and SOSM tracking performance is practically negligible.

TABLE III
RMS REFERENCE TRACKING ERRORS: STEER REVERSAL TEST AT 100 KM/H

E_{rms}	+300 kg	+200 kg	+100 kg	Nominal
IMC	$3.1 \cdot 10^{-3}$	$1.8 \cdot 10^{-3}$	$1.4 \cdot 10^{-3}$	$1.1 \cdot 10^{-3}$
SOSM	$3.5 \cdot 10^{-3}$	$2.1 \cdot 10^{-3}$	$1.8 \cdot 10^{-3}$	$1.8 \cdot 10^{-3}$

TABLE IV
STEER WHEEL FREQUENCY SWEEP AT 100 KM/H: BANDWIDTH AND RESONANCE PEAK VALUES

	Resonance Peak (dB)	Bandwidth (Hz)
Nominal uncontrolled	2.7	2.1
Nominal IMC	1.2	3
Nominal SOSM	0.9	2.3
Uncontrolled +300 kg	3.6	1.8
IMC +300 kg	2	2.5
SOSM +300 kg	2	1.9

C. Steering wheel frequency sweep

The steering wheel frequency sweep has been performed at 100 km/h in the frequency range 0-4 Hz, with a handwheel angle amplitude of 20°. The aim is to evaluate the bandwidth and resonance peak obtained with the considered control systems. In Table IV the simulated behaviour of the transfer ratio $T_m(\omega) = |\dot{\psi}(\omega)/|\ \dot{\psi}_{\text{ref}}(\omega)|$ is shown, putting into evidence the significant reduction of the resonance peak provided by the Sliding Mode controller. A slightly higher resonance peak, but also a higher system bandwidth, are obtained with the IMC controller in the nominal case. With the increased mass (+300 kg) vehicle, the same resonance peak is obtained. The controlled vehicle performs better than the uncontrolled one with both the considered control techniques.

D. Steering step plus lateral wind disturbance

This test aims to evaluate the system performances in presence of external disturbances. A steering step with handwheel angle of 40° at 110 km/h, with a steering wheel speed of 400°/s is performed. Then, at time instant $t = 3\,\text{s}$ a quite strong lateral wind (100 km/h) acts on the vehicle. Such a disturbance is modelled by a lateral force $F_{y,\text{wind}} = 800$ N plus an external yaw moment $M_{z,\text{wind}} = 500$ Nm, both applied on the vehicle centre of gravity. Fig. 12 shows the obtained results with the vehicle with increased mass (+300 kg): both control systems can reject the effects of the wind disturbance in an effective way, with practically the same behaviour. The obtained rms errors with changing vehicle mass are reported in Table V, showing that IMC control law performs slightly better than SOSM.

TABLE V
RMS REFERENCE TRACKING ERRORS: HANDWHEEL STEP AT 100 KM/H WITH LATERAL WIND

E_{rms}	+300 kg	+200 kg	+100 kg	Nominal
IMC	$2.4 \cdot 10^{-4}$	$2.0 \cdot 10^{-4}$	$1.9 \cdot 10^{-4}$	$1.8 \cdot 10^{-4}$
SOSM	$4.0 \cdot 10^{-4}$	$3.7 \cdot 10^{-4}$	$4.2 \cdot 10^{-4}$	$3.2 \cdot 10^{-4}$

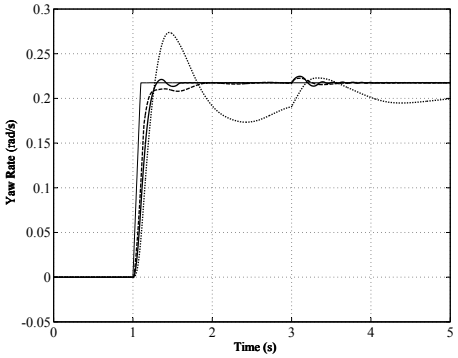

Fig. 12. 40° Handwheel step at 110 km/h in presence of lateral wind, increased mass (+ 300 kg) vehicle. Reference yaw rate course (thin solid line) and those obtained with the uncontrolled vehicle (dotted) and the controlled vehicles with Sliding Mode (solid) and IMC (dashed).

E. High speed braking in a turn

This test is employed by Mercedes to evaluate the performance of ESP® systems (see [27]). The maneuver starts at 200 km/h on a curve with constant radius R=1000 m. A braking action with constant longitudinal deceleration $\overline{a}_x$ is then performed and the maximum yaw rate deviation $\Delta\dot{\psi}$, with respect to the initial steady–state value, within the first second after the braking is evaluated. The test is performed with increasing values of longitudinal deceleration and the resulting curves $\Delta\dot{\psi}(\overline{a}_x)$ are plotted. Fig. 13 shows the results obtained with the increased mass (+300 kg) vehicle. Similar results are obtained with the nominal configuration. It can be noted

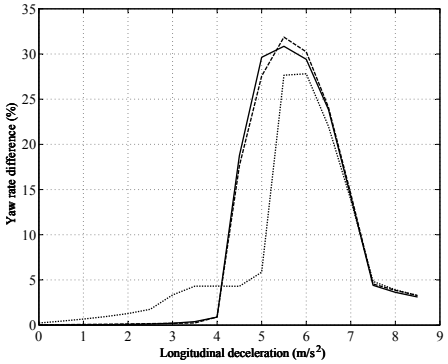

Fig. 13. High speed braking in a turn, yaw rate difference $\Delta\dot{\psi}(\overline{a}_x)$ for the increased mass (+300 kg) uncontrolled vehicle (dotted) and controlled vehicles with Sliding Mode (solid) and IMC (dashed) controllers.

that the IMC and Sliding Mode controlled vehicles show practically the same behaviour. Note that before a certain deceleration level (about 5.5 m/s^2 for the nominal vehicle and 4 m/s^2 for the increased mass one) the yaw rate deviation of the controlled vehicles is much lower than that of the uncontrolled one. Then, a sudden increase in $\Delta\dot{\psi}$ occurs for both the controlled vehicles, followed by a similar behaviour of the uncontrolled vehicle for even higher deceleration. This phenomenon is due to the fact that the particular stability system considered in this paper, i.e. a rear active differential, is not well-suited to counterbalance the excessive oversteer given by this maneuver and leads to worse results than the

uncontrolled vehicle. In fact, due to the interaction between tyre longitudinal and lateral forces, the intervention of the RAD may lead to saturate the lateral force at the rear wheels, thus exciting an oversteering behaviour instead of correcting it.

F. ISO double lane change

The aim of this maneuver is to test the effectiveness of the proposed approaches also in closed loop, i.e. in presence of the driver's action. The ISO double lane change maneuver has been implemented as reported in [28], with constant test speed $v_{\text{ref}} = 100\,\text{km/h}$. The reference vehicle path in terms of yaw angle $\psi_{\text{ref}}(t)$ is reported in Figure 14. The simple driver's

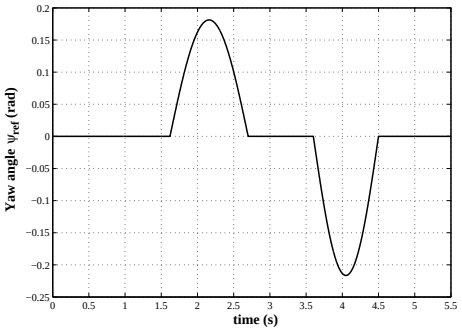

Fig. 14. Reference yaw angle $\psi_{\text{ref}}(t)$ for the ISO double lane change test at 100 km/h

model described e.g. in [28] has been used:

$$\delta(s) = \frac{K_d}{\tau_d\, s + 1}\left(\psi_{\text{ref}}(s) - \psi(s)\right)$$

More complex driver models could be employed, however the purpose of the considered closed loop maneuvers is to simply make a comparison between the handling properties of the uncontrolled vehicle and the controlled ones, given the same driver model. The values of the driver gain K_d and of the driver time constant τ_d have been chosen as $K_d = 0.63$ and $\tau_d = 0.16\,\text{s}$. Note that the values of τ_d range from $0.08\,\text{s}$ (experienced driver) to $0.25\,\text{s}$ (unexperienced driver), while the higher is the driver gain, the more aggressive is the driving action which could cause more likely vehicle instability. Fig. 15 shows the obtained results, considering the increased mass (+300 kg) vehicle, in terms of handwheel angle $\delta_H(t) = 15.4\,\delta(t)$: it can be noted that with both IMC and SOSM the resulting driver input is less oscillating than the one obtained in the uncontrolled case, showing again that the considered control strategies achieve quite good improvements of the system damping properties. Fig. 16 shows the obtained courses of the control variable M_z: once more it can be noted that the SOSM controller is less aggressive than IMC but it leads to practically the same results. On the other hand, chattering of the Sliding Mode control input is also evident in the final part of the maneuver.

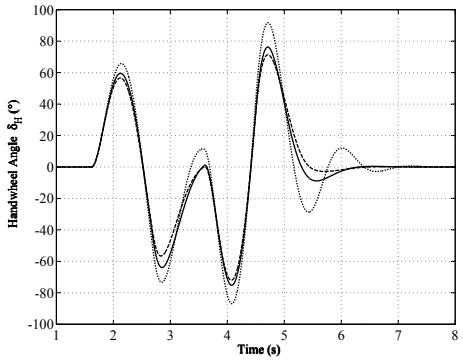

Fig. 15. ISO double lane change at 100 km/h, handwheel input δ_H for the increased mass (+300 kg) uncontrolled vehicle (dotted) and controlled vehicles with Sliding Mode (solid) and IMC (dashed)

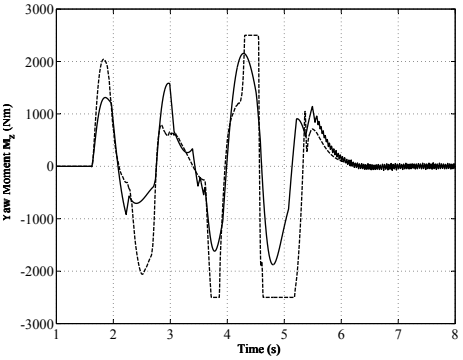

Fig. 16. ISO double lane change at 100 km/h, control input M_z for the increased mass (+300 kg) controlled vehicle with Sliding Mode (solid) and IMC (dashed)

VI. Conclusions and future perspectives

Control design based on Internal Model Control and Second Order Sliding Mode techniques has been presented, for the problem of vehicle yaw control. The performances obtained by the considered controllers have been compared using a detailed 14 d.o.f. vehicle model. Small reference tracking errors have been obtained with both controllers during steering pad maneuvers and good transient performances have been achieved in steer reversal tests. A slightly higher system bandwidth, but also a higher resonance peak, has been obtained by the IMC controller in the handwheel frequency sweep test. Quite good disturbance rejection properties and similar behaviours in oversteer contexts and closed loop lane change maneuvers have been shown. The robustness of the employed controllers has been also tested, since the considered maneuvers have been performed with varying vehicle speed and mass.Moreover, Sliding Mode control proved to be less aggressive with practically the same performances of the IMC controller. On the other hand, chattering of the control input is absent with the enhanced IMC controller, while it could be a serious issue in SOSM control. With both control techniques, stability in demanding oversteering conditions, like braking in a high speed turn, may be worse than the uncontrolled case, depending on the longitudinal deceleration level. This is due to the properties of the RAD, which is not well suited to stabilize the vehicle in such situations. Future works will aim to test stability and performance with low and non–uniform road friction coefficients and to compare the implementation issues of SOSM and IMC control laws, regarding required

sampling period and computational complexity. Moreover, the possibility of combining these techniques will be also investigated, in order to exploit their respective benefits in vehicle stability control.

REFERENCES

[1] J. Ackermann and W. Sienel, "Robust yaw damping of cars with front and rear wheel steering" *IEEE Trans. on Control Systems Technology*, vol. 1, no. 1, pp. 15–20, 1993.

[2] J. Ackermann, J. Guldner, R. Steinhausner and V. I. Utkin,"Linear and nonlinear design for robust automatic steering", *IEEE Trans. on Control System Technology*, vol. 3, no. 1, pp. 132–143, 1995.

[3] B. A. Güvenç, T. Bünte and L. Güvenç,"Robust two degree-of-freedom vehicle steering controller design", *IEEE Trans. on Control System Technology,* vol. 12, no. 4, pp. 627–636, 2004.

[4] J. E. Naranjo and C. González,"Power-Steering Control Architecture for Automatic Driving", *IEEE Trans. on Intelligent Transportation Systems* , vol. 6, no. 4, pp. 406–415, 2005.

[5] A. T. van Zanten, R. Erhart and G. Pfaff, "VDC, The vehicle dynamics control system of Bosch", *SAE Technical Paper no. 95759*, 1995.

[6] A. T. van Zanten, "Bosch ESP systems: 5 years of experience", *SAE Technical Paper no. 2000-01-1633*, 2000.

[7] M. A. Vilaplana, O. Mason, D. J. Leith, and W. E. Leithead "Control of Yaw Rate and Sideslip in 4-Wheel Steering Cars with Actuator Constraints" in *Lecture Notes in Computer Science*, vol. 3355, pp. 201–222, 2005.

[8] M. Canale, L. Fagiano, M. Milanese and P. Borodani, "Robust vehicle yaw control using an active differential and IMC techniques", *Control Engineering Practice*, no. 15, pp. 923–941, 2007.

[9] M. Morari, E. Zafiriou, *Robust Process Control,* Prentice Hall, 1989.

[10] A. Zheng, M.V. Kothare and M. Morari, "Anti-windup design for internal model control", *International Journal of Control*, vol. 60, no. 5, pp. 1015–1022, 1994.

[11] M. Canale, "Robust control from data in presence of input saturation", *International Journal of Robust and Nonlinear Control*, vol. 14, no. 11, pp. 983–998, 2004.

[12] V.I. Utkin, *Sliding Modes in Control and Optimization*, Springer–Verlag, New York, 1992.

[13] C. Edwards and K. S. Spurgeon, *Sliding Mode Control: Theory and Applications,* Taylor & Francis, London, UK, 1998.

[14] G. Bartolini, A. Ferrara, F. Levant and E. Usai, "On second order sliding mode controller," in *Variable Structure Systems, Sliding Mode and Nonlinear Control*, K–K. David Young and Ü. Özgüner Eds. Lecture Notes in Control and Information Sciences, Springer–Verlag, vol. 247, pp. 329–350, 1999.

[15] G. Bartolini, A. Ferrara and E. Usai,"Output tracking control of uncertain nonlinear second-order systems," *Automatica*, vol. 33, no. 12, pp.2203–2212, 1997.

[16] S. Data, F. Frigerio, "Objective evaluation of handling quality", *Journal of Automobile Engineering*, vol. 216, no. 4, pp. 297–305, 2002.

[17] R. Rajamani, *Vehicle Dynamics and Control*, New York: Springer, 2005

[18] L. Ippolito, G. Lupo and A. Lorenzini "System for controlling torque distribution motor vehicle differential", *Patent no. US 2002/0016661 A1*, Applicant Centro Ricerche Fiat, 1992.

[19] S. Frediani, R. Gianoglio and F. Giuliano "System for the active control of a between the wheels of a common vehicle axle", *EU Patent no. 92121621.4*, Applicant Centro Ricerche Fiat, 2002.

[20] E. Bakker, L. Lidner, H.B. Pacejka, "A New Tyre Model with an Application in Vehicle Dynamics Studies", *SAE Paper 890087*, 1989.

[21] D. C. Liaw, H. H. Chiang and T. T. Lee, "Elucidating Vehicle Lateral Dynamics Using a Bifurcation Analysis", *IEEE Trans. on Intelligent Transportation Systems* , vol. 8, no. 2, pp. 195–207, 2007.

[22] S. Skogestad and I. Postlethwaite, *Multivariable Feedback Control*, UK: Wiley, 2005.

[23] M. Milanese, M. Taragna, "H-infinity Set Membership Identification: a survey", *Automatica*, vol. 41, no. 12, pp. 2019-2032, ISSN: 0005-1098, 2005.

[24] A. F. Filippov, *Differential Equations with Discontinuous Right–Hand Side*. Kluwer, Dordrecht, the Netherlands, 1988.

[25] A. Levant and L. Fridman, "Higher order sliding modes," in *Sliding Mode Control in Engineering*, Wilfrid Perruquetti and Jean-Pierre Barbot Eds. Marcel Dekker Inc., New York, NY, pp. 53–101, 2002.

[26] I. Boiko, L. Fridman, A. Pisano and E. Usai, "Analysis of Chattering in Systems With Second-Order Sliding Modes," *IEEE Trans. on Automatic Control*, vol. 52, no. 11, pp. 2085–2102, 2007.

[27] M. Nuessle, R. Rutz, M. Leucht, M. Nonnenmacher and H. Volk, "Objective test methods to assess active safety benefits of ESP" in *20^{th} International Technical Conference on the Enhanced Safety of Vehicles (ESV)*, paper no. 07-0230, Lyon, France, 2007.

[28] G. Genta, *Motor Vehicle Dynamics, II ed.* (World Scientific), 2003.